# Cooperative Behavior of $K^+$ Channels in the Tonoplast of *Chara corallina*

Silke Draber, Roland Schultze, and Ulf-Peter Hansen
Institut für Angewandte Physik der Universität Kiel, Kiel, Germany

ABSTRACT Spontaneous cooperativity of $K^+$ channels is studied in excised patches of *Chara corallina* tonoplasts. Bar histograms (dwell time versus number of open channels) are constructed from the time series of current by means of the higher-order Hinkley detector (R. Schultze and S. Draber. 1993. *J. Membr. Biol.* 132:41–52). A statistical test, based on these bar histograms, shows that the channels are not independent. Further analysis reveals that the channels are cooperatively changing their open probability, which leads to the idea of cooperative mode shifting.

## INTRODUCTION

The patch-clamp technique makes possible the measurement of current through individual ion transport channels. In most studies it is assumed that channels behave independently. However, the cooperativity of channels in biological membranes has been investigated by several workers (Kiss and Nagy, 1985; Iwasa et al., 1986; Yeramian et al., 1986; Manivannan et al., 1992).

The observations presented in this paper lead us to a combination of the idea of cooperativity with the idea of mode shifting. Mode shifting, the phenomenon that a single channel switches between two or three distinct "modes" of gating, characterized by different open probabilities, has been reported from the dihydropyridine-sensitive N-type $Ca^{2+}$ channel (Hess et al., 1984), the L-type $Ca^{2+}$ channel (Plummer and Hess, 1991), and the $\mu$I $Na^+$ channel (Zhou et al., 1991).

Cooperativity and mode shifting have been discussed separately until now.

## MATERIALS AND METHODS

The experimental set-up and the procedure of obtaining cytoplasmic droplets have been described by Draber et al. (1991). Briefly, cells of *Chara corallina*, grown in artificial pond water (0.1 mM KCl, 1.0 mM NaCl, 0.1 mM $CaCl_2$), were cut, and the cytosol was released into a petri dish. In the bathing solution of 250 mM KCl and 5 mM $CaCl_2$, vescicles with a diameter of ~50 $\mu$m were formed. The outer membrane of these vesicles has been shown to consist of tonoplast fragments (Bertl, 1989; Lühring, 1986; Sakano and Tazawa, 1986).

Patch electrodes were pulled from borosilicate glass (AR-type; Hilgenberg, Malsberg, Germany) with a L/M-3P-A puller (List Electronic, Darmstadt, Germany), coated with Sylgard (Dow Corning), fire polished, and filled with the bathing solution (250 mM KCl and 5 mM $CaCl_2$).

In order to exclude synchronization of channel behavior by metabolic signals, the investigations were made in the excised configuration (inside out). The membrane potential was set to different voltages between +200 mV and −150 mV by means of a patch-clamp amplifier (EPC-7; List Electronic) and kept constant for about 2 min. The current was obtained at constant voltage during the second minute. For antialiasing it was low-pass filtered with a tunable 8-pole switched capacitor Bessel filter (LTC 1064; Linear Technology) set to a cutoff frequency (−3 dB) of 25 kHz. The current signal was sampled at 100 kHz and stored on a 676-megabyte hard disk for off-line analysis.

*Received for publication 30 November 1992 and in final form 19 July 1993.*
Address reprint requests to Dr. Silke Draber, Institut für Angewandte Physik der Universität Kiel, D-24098 Kiel, Germany.

0006-3495/93/10/1553/07 $2.00

## THEORY

Given an ensemble of $N$ independent and identical channels, the probability $b(i)$ that $i$ channels are open (and $N - i$ are closed) is described by a binomial distribution

$$b(i) = \frac{N!}{(N-1)! \cdot i!} \cdot p_{\text{open}}^{i} \cdot (1 - p_{\text{open}})^{N-i} \qquad (1)$$

In a measurement with duration $S$ the expected values $B_i$ of the time with $i$ channels open therefore are

$$B_i = S \cdot b(i) = S \cdot \frac{N!}{(N-i)! \cdot i!} \cdot p_{\text{open}}^{i} \cdot (1 - p_{\text{open}})^{N-i} \qquad (2)$$

A popular way to decide whether the observed channels are independent and identical is to compare the theoretical distribution $B_i$ with the measured distribution $M_i$ of dwell times at level $i$ and to perform a test to determine whether the differences between $M_i$ and $B_i$ are statistically significant. In this paper we propose new methods for both tasks: first, determination of the measured distribution $M_i$ and second, testing for differences between theory and experiment.

### Determination of $M_i$, the total dwell time at level $i$

In an idealized noise-free time series of pipette current, $M_i$ is the total time in which the current signal dwells at level $i$. By means of strong filtering (500 Hz) Iwasa et al. (1986) have removed noise from the time series so that they have been able to determine $M_i$ directly. This procedure is restricted to very slow gating. Otherwise the strong filtering would remove a substantial amount of open or closed events. Therefore, the determination of $M_i$ is not as simple in most cases.

Manivannan et al. (1992) have used amplitude histograms like that in Fig. 1 *B*. They have obtained the times $M_i$ from the area of Gaussian distributions fitted to an amplitude histogram. However, this kind of fit cannot be applied if very

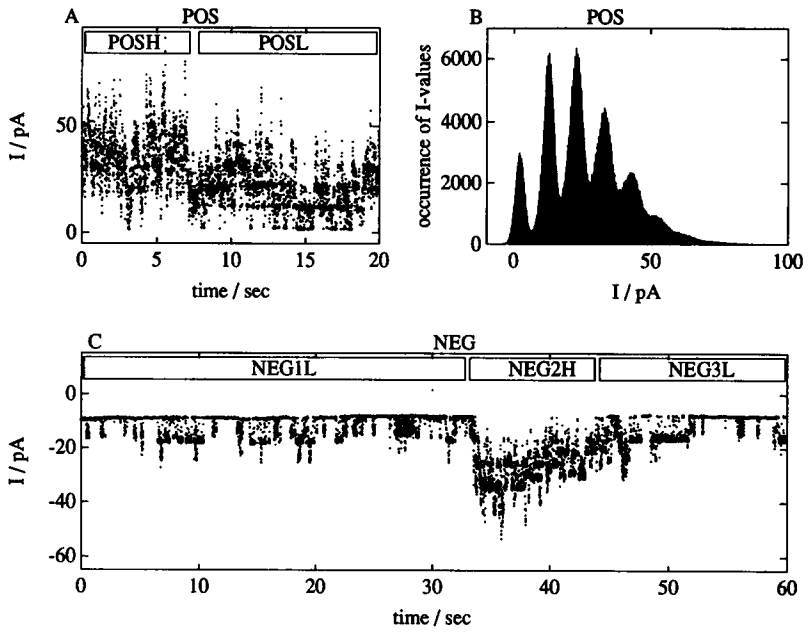


FIGURE 1 Experimental time series of pipette current from tonoplast vesicles of *Chara* in excised-patch configuration in a solution of 250 mM KCl, 5 mM $CaCl_2$. (*A*) time series POS (2,000,000 samples, 20 s) at positive voltage $V = 60$mV, resulting in a single-channel current of 10.5 pA. There are at least seven channels within the patch. They do not behave independently. For the display in this figure the time series was low-pass filtered with 250 Hz. The time series is divided into a part POSH with high open probability and a part POSL with low open probability. (*B*) amplitude histogram of the unfiltered time series. The occurence of the current values is plotted versus the *I*-axis, which is divided into units of the AD converter (0.056 pA). (*C*) time series NEG (6,000,000 samples, 60 s). The voltage of $V = -86$mV drives a single-channel current of −9.2 pA. There are five channels within the patch, which behave cooperatively. The time series is divided into three parts, NEG1L, NEG2H, and NEG3L (see Table 1 for the statistical results).

fast switching events convert the gaussian distributions into beta distributions (Yellen, 1984).

To circumvent this problem, we apply the higher-order Hinkley detector (Schultze and Draber, 1993) to the time series and obtain dwell-time histograms (Fig. 5) for every level $i$. The sum of the dwell times gives $M_i$. The experimental result of $M_i$ versus $i$ can be depicted as a bar histogram (Fig. 2).

## Testing the independence of channels

The theoretical distribution $B_i$ (Eq. 2) depends on three parameters: the total recording time $S$, the open probability $p_{\text{open}}$, and the number $N$ of channels. These parameters must be determined from the experiment. First, we discuss the testing problem under the assumption that the number $N$ of channels in the patch is known. The information from the experiment is condensed into the $N + 1$ bars $M_i$ ($i = 0, \ldots, N$). The parameters $S$ and $p_{\text{open}}$ are determined by the following equations:

$$S = \sum_{i=0}^{N} M_i \tag{3}$$

$$p_{\text{open}} = \frac{1}{S \cdot N} \sum_{i=0}^{N} i \cdot M_i \tag{4}$$

With the knowledge of $N$, $S$, $p_{\text{open}}$ it is possible to calculate the theoretical distribution $B_i$ according to Eq. 2. The differences between $B_i$ and $M_i$ are used for a statistical test that decides whether they are significant or have occurred just by chance. Before applying a test it is instructive to consider the degrees of freedom, that is, the dimension of the space of deviations between $B_i$ and $M_i$. Starting from the $(N + 1)$-dimensional space of the bars $M_0, M_1, \ldots, M_N$, two degrees of freedom are used to determine $S$ and $p_{\text{open}}$ (Eqs. 3 and 4). Thus, there are only $F = (N + 1) -$

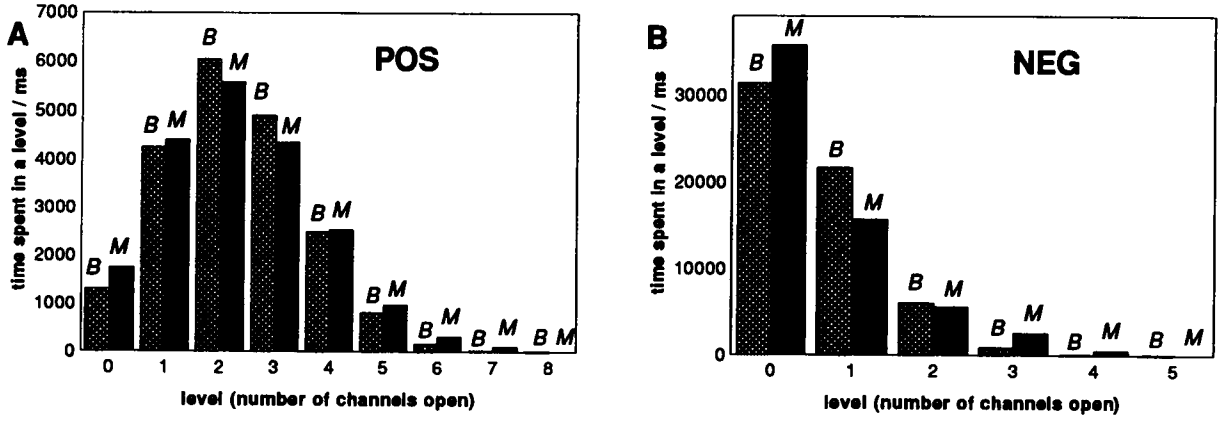


FIGURE 2 Bar histograms of the whole records in Fig. 1. The bars present the time spent in one level of current, as reconstructed by the higher-order Hinkley detector (*M*). The *B* columns indicate the best binomial fit to the measured (*M*) data. The binomial fits fail.

$2 = N - 1$ degrees of freedom left that can be used to decide whether $M_i$ differs significantly from $B_i$. If $N = 1$ the theory perfectly fits the data, which is indicated by $F = 0$ degrees of freedom. If $N = 2$ the statistical test has to be based on a one-dimensional variable ($F = 1$). Using the test variable $\Delta = (M_1)^2/(M_0 \cdot M_2)$ proposed by Manivannan et al. (1992) or the ratio of measured to theoretical variance as recommended by Liu and Dilger (1993) is essentially equivalent in that case. The situation changes, if more than two channels offer the possibility of using more than one degree of freedom and making the test more reliable. To accomplish this we use a $\chi^2$ test.

The statistical test must take into account the consideration that the time series is correlated. A temporal unit $T$ is introduced that represents the inherent correlation of the data. This is roughly the slowest time constant of gating. In our case $T = 10$ ms has been used for records at positive potentials and $T = 50$ ms for negative potentials. Since (for fixed $i$) the scaled number $M_i/T$ counts independent observations, it is viewed as the realization of a random variable being Poisson distributed with mean (and variance) $B_i/T$. After $\chi^2 = \sum_{i=0}^{N} (B_i/T - M_i/T)^2/(B_i/T)$ is calculated, $\chi^2/F$ is compared with the threshold value (max. in Table 1) taken from a standard table of statistics (e.g., Sachs, 1984) for a significance level of 5%. If $\chi^2/F$ exceeds this greatest allowed value, the distribution $M_i$ is said not to be binomial.

### Determination of *N*

In practice the number $N$ of channels is not known a priori. It is only possible to quantify $N \geq N_{obs}$, where $N_{obs}$ is the observed number of simultaneously open channels in the time series. Horn (1991) has discussed various methods for the determination of $N$. As in our previous paper (Draber et al., 1991) we perform the $\chi^2$ test based on different $N = N_{obs}, N_{obs} + 1, \ldots$, which allows the determination of $N$ along with the statistical test for cooperativity. The number $N$ of channels with the smallest value of $\chi^2/F$ is assumed to be correct.

**TABLE 1 Statistical results of the three examples POS, NEG, and SIM in whole and in sections**

| | $N$ | $p_{open}$ | $\chi^2/F$ | max | Binomial |
|---|---|---|---|---|---|
| POS | 8 | 0.29 | 7.79 | 2.01 | No |
| POSH | 8 | 0.41 | 1.04 | 2.01 | Yes |
| POSL | 8 | 0.22 | 0.19 | 2.01 | Yes |
| NEG | 5 | 0.12 | 32.32 | 2.37 | No |
| NEG1L | 5 | 0.05 | 0.81 | 2.37 | Yes |
| NEG2H | 5 | 0.47 | 1.28 | 2.37 | Yes |
| NEG3L | 5 | 0.08 | 0.70 | 2.37 | Yes |
| SIM | 8 | 0.29 | 44.38 | 2.01 | No |
| SIM1H | 8 | 0.39 | 0.47 | 2.01 | Yes |
| SIM2L | 8 | 0.21 | 0.39 | 2.01 | Yes |
| SIM3H | 8 | 0.42 | 0.81 | 2.01 | Yes |
| SIM4L | 8 | 0.23 | 0.37 | 2.01 | Yes |

SIM is a simulation (Fig. 8). $N, p_{open}$ are the parameters of the fitted binomial distribution. The comparison of the $\chi^2/F$ value with its upper threshold (max) results in the acceptance or rejection of a binomial distribution (last column).

## RESULTS

In patches containing multiple channels, an effect of cooperativity is observed. Fig. 1 shows the phenomenon that was sometimes observed in records of pipette current. Two examples are given—one for positive and one for negative potentials. The boxes above the current trace indicate the sections of high and low open probability separated by sudden changes of channel behavior.

### Testing independence in the whole record and in the sections

As described under Theory, bar histograms (Fig. 2) can be used for checking the independence of channels. The results of the fitting procedure and of the statistical tests are shown in Table 1. The binomial fit of the histograms in Fig. 2 fails (see also first and fourth rows of Table 1). The fitted binomial distributions ($B_i$) give systematically less time spent in the higher levels (e.g., 5, 6, 7 in Fig. 2 *A*) than is measured in the experiment ($M_i$). The test variable $\chi^2/F$ is much higher than the greatest allowed value (max) for a binomial distribution. This leads to the conclusion that the channels do not behave independently.

In contrast to the whole records, independence is found if the time series are divided into sections POSH and POSL in Fig. 1 *A* and NEG1L, NEG2H, and NEG3L in Fig. 1 *C*. Histograms are obtained that can be fitted by a binomial approach. The test variables $\chi^2/F$ for the sections are below the allowed threshold and are smaller by a factor of ten than for the whole record (see Table 1). Fig. 3 shows the fits for POSH and POSL. The results of the statistical analysis for both examples POS and NEG are given in the first seven rows of Table 1. In the experiment POS of Fig. 1 *A*, the open probability switches from 0.41 in the first part POSH (high) down to 0.22 in the second part POSL (low). In the experiment NEG of Fig. 1 *C*, it changes from 0.05 (NEG1L) to 0.47 (NEG2H) and back to 0.08 (NEG3L).

### Constancy of channel number at a sudden change of open probability

The observed differences between the sections of the records in Fig. 1 lead to the question: What has changed? The most important finding concerns the number of channels. The binomial fit results in a number of $N = 8$ ($N_{obs} = 7$) for the positive record in both sections (see minima in Fig. 4). A number of $N = 5$ was determined for all three sections of the negative record. In contrast, the number of channels cannot be determined from the whole records POS and NEG. If we apply the test for the selection of the parameter $N$ to the total time series, we get the nonsensical result $N \rightarrow \infty$ (Fig. 4) as an additional indication that the binomial distribution does not fit. Of course, for the calculation of the statistical values in Table 1 we have used the same number $N$ for the whole records as we have for the sections.

The fact that the number of channels has not changed between the sections POSH and POSL is obvious from the clear

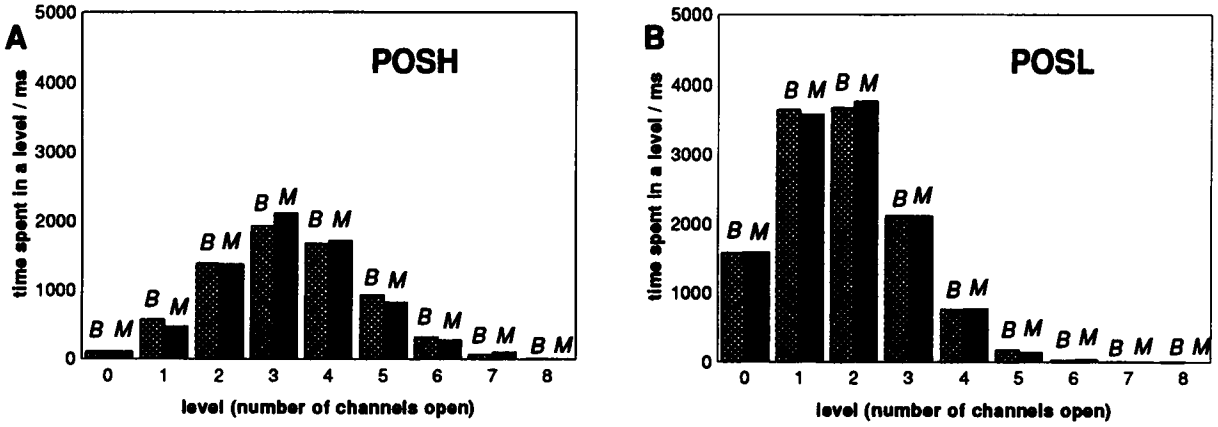


FIGURE 3 Bar histograms from the two sections of measurement POS (in Fig. 1). (*A*) POSH: The $\chi^2$ test confirms that the bars are binomially distributed with a high open probability $p_{open} = 0.41$. (*B*) POSL: binomial, low $p_{open} = 0.22$ (see Table 1 for statistical details).

FIGURE 4 The test variable $\chi^2/F$ versus the assumed number $N$ of channels. (*A*) POS: The minimum of $\chi^2/F$ in both sections POSH and POSL is obviously $N = 8$. The dashed line shows the maximally allowed test value for a significance level of 5%. According to this test the bar histogram of the whole record POS is not binomially distributed. (*B*) NEG: The minima of $\chi^2/F$ at $N = 5$ channels are not as obvious as in (*A*). This is due mainly to the small open probability of NEG1L and NEG3L, which reduces the differences between the binomial distributions related to different numbers $N$.

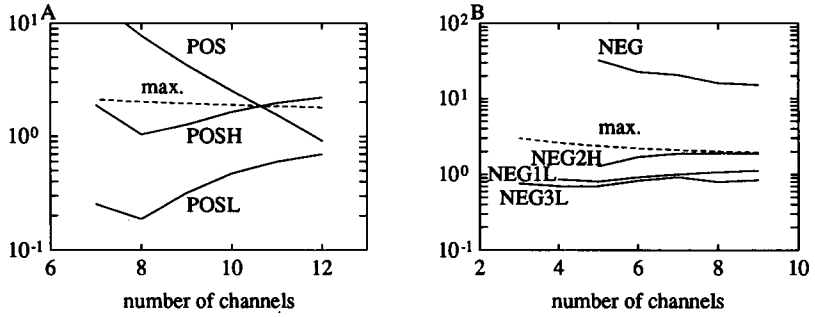


minimum in Fig. 4 *A*. However, the curves in Fig. 4 *B* show a less significant minimum (five channels). This is due to the small open probability that drives the binominal distributions of NEG1L and NEG3L nearer to a Poisson distribution, and this handicaps the determination of $N$. Nevertheless, the measurements cannot be explained simply by a change of the number $N$ of channels without a change in open probability. This is supported for the less significant case of NEG by the following argument. The ratio of $N \cdot p_{open}$ between the high and low sections of NEG is about 7. The number $N$ is at least 2 in the low sections (see Fig. 1 *C*). Since it is very unlikely that the number $N$ of channels has changed from 2 to 14 and back to 2, a change in open probability and not in the number of channels explains the data much better.

## Gating model

According to the analysis above, the regions of different activity in Fig. 1 (*A* and *C*) show a sudden change in open probability without a change in the number of channels involved. To verify this result and to find out which transition(s) of a gating model are affected by mode shifting, the following analysis is made. For the determination of the gating model, two problems must be solved: reconstruction of the time series without noise and handling the problems of multichannel analysis and of missed events.

### *Dwell-time histograms created by the higher-order Hinkley detector*

The higher-order Hinkley detector reconstructs the noise-free time series. The detected events can be classified by their level $l = 0, \ldots, N_{obs}$ and by their type of time course, as illustrated by the following symbols: ⌐¬, open; ⊔, closed; ⌐⊣ and ⊢¬, transient. In our case of flickering channels, the transient events are rare. Therefore, we lump them with the open and closed events in the following way. In Fig. 5 open events comprise ⌐¬, and ⌐⊣, and closed events ⊔, and ⊢¬. We generate $N_{obs}$ dwell-time histograms of open events (for level 1 to $N_{obs}$) and $N_{obs}$ histograms for closed events (level 0 to $N_{obs} - 1$). Fig. 5 shows the result of section POSL, which is quite typical for the $K^+$ channel of *Chara*: the shape of the closed-time histograms is nearly the same for all levels. The shape of the open-time histograms is different for different levels. On average, open events at a high level are shorter than open events at a low level.

### *Multichannel analysis*

We have developed a special method for the analysis of multilevel dwell-time histograms based on the concept of burst kinetics. A single channel is either in a long-living closed state (*C*) or "flickering," that is, open (*O*) but interrupted by frequent but very short closures or so-called gaps (*G*). When

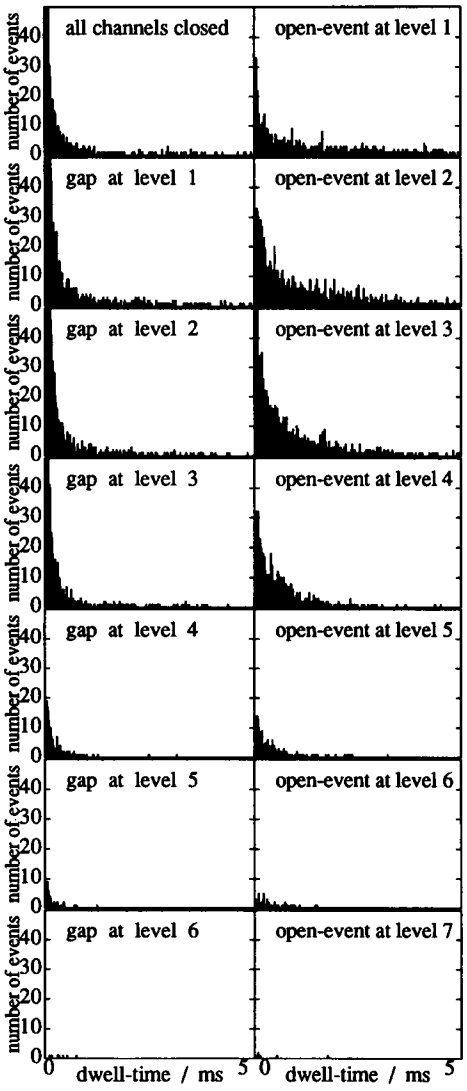


FIGURE 5 Dwell-time histograms for open events and closed events (gaps) on multiple levels of the record POSL. The time axis ends at 5 ms. Longer events are not displayed.

$l$ channels are flickering and all other channels are closed, the signal switches between level $l$ and $l - 1$. Due to their short duration, gaps rarely occur simultaneously. This behavior, as presented schematically in Fig. 6, has two consequences: (*a*) The closed events at all levels are single gaps. The dwell-time distribution is the same as in the single-channel case. (*b*) The frequency of gaps, however, is $l$ times higher than in the single-channel case. The dwell time of open events at level $l$ is therefore shorter by a factor $1/l$ than the dwell time of open events at level 1. An exponential joint fit of all open-time histograms with the time constant $\tau_O/l$ for level $l$ gives a good fit and agrees with a free fit, which supports the developed theory. For the open-time histograms in Fig. 5 the result is $\tau_O = 2.28$ ms. A second, very fast time constant seems to be in the open-time histograms, which is especially obvious at level 1 in Fig. 5. This is an artifact, arising from overlapping gaps from level 2 down to the baseline and back to level 2, which produce two transient events ( ⊢, ⊣ ) at level 1. The first of them is counted as "open event," which explains the fast time constant of open events as an artifact.

The joint fit of the closed-time histograms with a single exponential fails and shows that there are two kinds of gaps involved at all levels. A joint fit with two time constants gives $\tau_{Gf} = 22.2$ $\mu$s for the predominant component of fast gaps $G_f$ and $\tau_{Gs} = 103$ $\mu$s for the second component of slow gaps $G_s$. This is in agreement with the time constants determined by a free fit.

The long-living closed state $C$ is visible only at level 0 (Jackson, 1985) when all channels are closed and none is flickering (see the time series in Fig. 1 *A*). Since the time axis of 5 ms in Fig. 5 is too short for the identification of the long-living closed state, we first reduce the sampling frequency of the time series by a factor of 20 by means of averaging blocks of 20 samples. From this record the higher-order Hinkley detector constructs the dwell-time histogram in Fig. 7 for the closed level 0. As is already obvious from the time series, there are only a small number of these long-lasting closed events, with a duration of up to 65 ms. The mean duration is approximately 31 ms. Since we know that eight channels are simultaneously closed in that state, the single-channel rate constant of opening is $k_{CO} = 1/(8 \cdot 31 \text{ ms}) \approx 4.0 \text{ s}^{-1}$.

### *Gating scheme*

The number of exponentials used for fitting leads to the structure of the gating scheme. It has to consist of one open state, one (long) closed state, and two (short) closed states for the gaps. As Kienker (1989) has shown there are many equivalent possible arrangements of these four states. We choose the simplest one, which offers the advantage that all transitions

FIGURE 6 Bursting channels. This plot illustrates the multichannel analysis. Gaps are short and do not occur simultaneously. The frequency of gaps is proportional to the number of flickering channels.

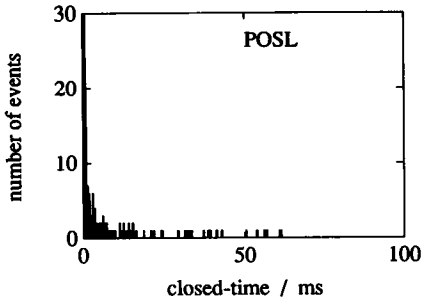


FIGURE 7 Closed-time histogram at level 0 (baseline) of record POSL on a longer time axis. There are some long events occurring in situations when all channels are closed.

change the channel conductance:

$$C \underset{k_{OC}}{\overset{k_{CO}}{\rightleftharpoons}} O \underset{k_{GfO}}{\overset{k_{OGf}}{\rightleftharpoons}} G_f \qquad k_{GsO} \uparrow\downarrow k_{OGs} \qquad G_s \tag{5}$$

### Missed events

When calculating the rate constants $k$ from time constants $\tau$, a correction for missed events must be performed which takes into account the final temporal resolution $t_{res}$ of the detector (Colquhoun and Sigworth, 1983; Blatz and Magleby, 1986; Milne et al., 1989; Crouzy and Sigworth, 1990). In our case of the flickering $K^+$ channel we are faced with a situation in which the missed gaps lead to a significant prolongation of the apparent lifetime in the open state. The lifetime of the gaps, however, is nearly correct since the open events are long enough to be detected. Application of the equation given by Colqhoun and Sigworth (1983) with $t_{res}$ = 30 $\mu$s to the time constants $\tau_O$ = 2.28 ms, $\tau_{Gf}$ = 22.2 $\mu$s determined above, results in the sum of the rate constants $k_{OC} + k_{OGs} + k_{OGf}$ = 1993 $s^{-1} \approx$ 2000 $s^{-1}$ for the open state, which is a significant correction compared with the simple inverse of the fitted time constant, namely $1/\tau_O$ = 439 $s^{-1}$. The corrected rate constant $k_{GfO}$ = 49,875 $s^{-1} \approx$ 50,000 $s^{-1}$ for the fast gap is quite close to $1/\tau_{Gf}$ = 45,000 $s^{-1}$. The opening rate constant $k_{GsO}$ from the slow gap is therefore approximately obtained by inversion of the time constant without correction for missed openings $k_{GsO} \approx 1/\text{tau}_{Gs}$ = 9,709 $s^{-1} \approx$ 10,000 $s^{-1}$.

### Closing rates

Until now we have determined only the total closing rate constant $k_{OC} + k_{OGs} + k_{OGf}$ = 2000 $s^{-1}$. The remaining problem is to decide what part of closures end in a fast gap $G_f$ and what part in a slow gap $G_s$. The small amount of closures to $C$ may be neglected for the moment because $k_{OC} \ll k_{OC} + k_{OGs} + k_{OGf}$. A possible approach is to determine the areas below the exponential functions fitted to the closed-time histograms. This assigns 25% (±5%) of the closed events to $G_s$ and 75% (±5%) to $G_f$, which leads to $k_{OGs}$ = 500 $s^{-1}$ and $k_{OGf}$ = 1500 $s^{-1}$.

The rate constant $k_{OC}$ of transitions into the long-lasting closed state, which was neglected above, is finally calculated from the open probability $p_{open}$ by means of the steady-state solution of the gating model. For the record POSL the open probability of $p_{open}$ = 0.22 implies $k_{OC}$ = 14.0 $s^{-1}$.

The final result of the record POSL is shown in the right box of Eq. 6. The left box shows the results of the section POSH with the high open probability. The difference in $k_{CO}$ reveals the rate constant, which is subject to changes caused by cooperative mode shifting:

Configuration H Configuration L

$$\begin{array}{c} k_{CO}=10.3s^{-1} \quad 1500s^{-1} \\ C \rightleftharpoons O \rightleftharpoons G_f \\ k_{OC}=14.0s^{-1} \quad 50000s^{-1} \\ 10000s^{-1} \uparrow\downarrow 500s^{-1} \\ G_s \end{array} \rightleftharpoons \begin{array}{c} k_{CO}=4.0s^{-1} \quad 1500s^{-1} \\ C \rightleftharpoons O \rightleftharpoons G_f \\ k_{OC}=14.0s^{-1} \quad 50000s^{-1} \\ 10000s^{-1} \uparrow\downarrow 500s^{-1} \\ G_s \end{array} \tag{6}$$

The presented method of evaluating multichannel dwell-time histograms is straightforward but neglects a number of considerations, which may give rise to errors in the final rate constants. Therefore the results must be tested by simulation. We have analyzed many simulated time series like that in Fig. 8 based on Eq. 6 above. Now a direct comparison of amplitude histograms and dwell-time histograms, including the exponential fits, is possible. These simulations reproduce the measured data very well, even the artifact of the fast exponential in the open-time histogram of level 1. The random scattering of the results from eight simulations and other measurements at positive voltage show that the error of the rate constants in the gating scheme (Eq. 6) is less than 30%. The analysis of the records obtained at negative potentials yields a similar result. The different value of $k_{CO}$ = 1.1 $s^{-1}$ at negative potentials instead of $k_{CO}$ = 4.0 $s^{-1}$ at positive potentials shows the voltage dependence of this rate constant. This is in line with the findings of Draber et al. (1991).

For all measurements, the calculation of rate constants shows that the change in open probability observed in Fig. 1 results from a change in a single rate constant $k_{CO}$, which determines the dwell time in the slow closed state $C$. The fast gap kinetics remain unchanged in both configurations.

## DISCUSSION

This paper presents results about the cooperative mode shifting of $K^+$ channels in *Chara corallina* and methods for analyzing cooperative behavior.

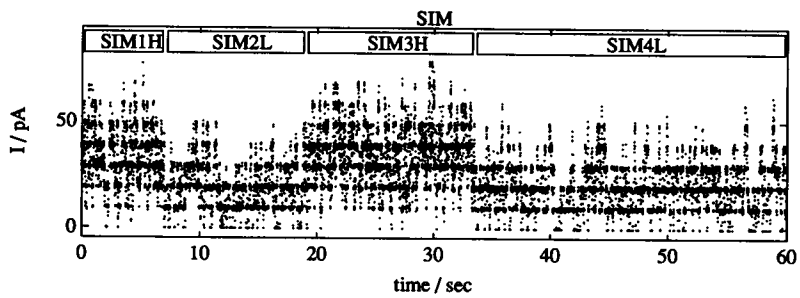


FIGURE 8 Simulated time series SIM (6,000,000 samples, 60 s) of eight channels, which show synchronous mode shifting between high and low open probability. The statistical results of the whole record and the four sections are listed in Table 1.

The new result on cooperativity concerns the phenomenon of cooperative mode shifting, which is different from the type of cooperativity found, for instance, by Iwasa et al. (1986) or Manivannan et al. (1992). Iwasa et al. (1986) have explained the interactions between cooperative $Na^+$ channels by an influence on the opening rate: a closed channel is more likely to stay closed if another channel is already open. Since the gating scheme of the channel is directly affected by the gating state (open or closed) of another channel, this is a mechanism of cooperative gating. It results in a stationary pattern of the time series of pipette current, which cannot be explained by independent identical channels, whether in whole or in isolated segments.

The cooperativity of the investigated $K^+$ channels of *Chara* is fundamentally different. Channels stay in modes of low or high open probability for some seconds. The transitions between these phases of high and low open probability occur simultaneously in all channels of the patch. This kind of cooperativity can be understood as cooperative mode shifting.

We interpret this kinetic observation as a consequence of interactions between channels. However, one might assume that these changes could emerge from an experimentally unobserved process such as metabolic signals from the cell. Although we cannot exclude the possibility that membrane-bound regulators still have an influence on the channel, the excised-patch configuration interrupts the main metabolic pathway from the cytoplasm to the membrane.

A molecular interpretation for the observed cooperativity can be based on the notion of channel clusters, which are so closely connected in the membrane that changes in the structure (open probability) of one molecule induce the same structural change in a neighboring molecule. Many types of channels occur in clusters. In the case of gap junction channels where cooperativity has been observed by Manivannan et al. (1992), Kensler et al. (1979) have found by freeze-fracture techniques that the channels occur in large clusters of about 100. Further evidence is given by the number of channels found within a patch. Very similar to the experience of Manivannan et al. (1992) is our finding that patches of the *Chara* tonoplast contain either no $K^+$ channel or, if there are some, more than three active channels. A typical value is six channels in the patch area of about 10 $\mu m^2$. This offers the possibility of explaining the cooperative behavior of the channels by postulating a kind of mechanical interaction between the neighboring channel proteins.

We thank Dipl.-Phys. Christian Ruge for many helpful discussions about a possible connection between cooperative channel dynamics and percolation structures in Ising models.

The experimental investigations were supported by the Deutsche Forschungsgemeinschaft (Ha 712/7-5).

## REFERENCES

Bertl, A. 1989. Current-voltage relationships of a sodium-sensitive potassium channel in the tonoplast of *Chara corallina*. *J. Membr. Biol.* 109: 9–19.

Blatz, A. L., and K. L. Magleby. 1986. Correcting single channel data for missed events. *Biophys. J.* 49:967–980.

Colquhoun, D., and F. J. Sigworth. 1983. Fitting and statistical analysis of single channel records. *In* Single-Channel Recording. B. Sakmann and E. Neher, editors. Plenum Press, New York, London. 191–263.

Crouzy, S. C., and F. J. Sigworth. 1990. Yet another approach to the dwell-time omission problem of single-channel analysis. *Biophys. J.* 58:731–743.

Draber, S., R. Schultze, and U-P. Hansen. 1991. Patch-clamp studies on the anomalous mole fraction effect of the $K^+$-channel in cytoplasmic droplets of *Nitella*: an attempt to distinguish between a multi-ion single-file pore and an enzyme kinetic model with lazy state. *J. Membr. Biol.* 123: 183–190.

Hess, P., J. B. Lansman, and R. W. Tsien. 1984. Different modes of Ca channel gating behaviour favoured by dihydropyridine Ca agonists and antagonists. *Nature (Lond.).* 311:538–544.

Horn, R. 1991. Estimating the number of channels in patch recordings. *Biophys. J.* 60:433–439.

Iwasa, K., G. Ehrenstein, N. Moran, and M. Jia. 1986. Evidence for interactions between batrachotoxin-modified channels in hybrid neuroblastoma cells. *Biophys. J.* 50:531–537.

Jackson, M. B. 1985. Stochastic behavior of a many-channel membrane system. *Biophys. J.* 47:129–137.

Kensler, R. W., P. R. Brink, and M. M. Dewey. 1979. The septum of the lateral axon of the earthworm: a thin section and freeze fracture study. *J. Neurocytol.* 8:565–590.

Kienker, P. 1989. Equivalence of aggregated Markov models of ion-channel gating. *Proc. R. Soc. Lond. Biol.* 236:269–309.

Kiss, T., and K. Nagy. 1985. Interaction between sodium channels in mouse neuroblastoma cells. *Eur. Biophys. J.* 12:13–18.

Liu, Y., and J. P. Dilger. 1993. Application of the one- and two-dimensional Ising models to studies of cooperativity between ion channels. *Biophys. J.* 64:26–35.

Lühring, H. E. 1986. Recording of single $K^+$ channels in the membrane of cytoplasmic drop of *Chara australis*. *Protoplasma.* 133:19–28.

Manivannan, K., S. V. Ramanan, R. T. Mathias, and P. R. Brink. 1992. Multichannel recordings from membranes which contain gap junctions. *Biophys. J.* 61:216–227.

Milne, R. K., G. F. Yeo, B. W. Madsen, and R. O. Edeson. 1989. Estimation of single channel kinetic parameters from data subject to limited time resolution. *Biophys. J.* 55:673–676.

Plummer, M., and P. Hess. 1991. Reversible uncoupling of inactivation in N-type calcium channels. *Nature (Lond.).* 351:657–659.

Sachs, L. 1984. Applied Statistics. Springer-Verlag, New York, Berlin, Heildelberg, Tokyo.

Sakano, K., and M. Tazawa. 1986. Tonoplast origin of the envelope membrane of cytoplasmic droplets prepared from *Chara* internodal cells. *Protoplasma.* 131:247–249.

Schultze, R., and S. Draber. 1993. A nonlinear filter algorithm for the detection of jumps in patch-clamp data. *J. Membr. Biol.* 132:41–52.

Yellen, G. 1984. Ionic permeation and blockade in $Ca^{2+}$-activated $K^+$ channels of bovine chromaffin cells. *J. Gen. Physiol.* 84:157–186.

Yeramian, E., A. Trautmann, and P. Claverie. 1986. Acetylcholine receptors are not functionally independent. *Biophys. J.* 50:253–263.

Zhou, J., J. F. Potts, J. S. Trimmer, W. S. Agnew, and F. J. Sigworth. 1991. Multiple gating modes and the effect of modulating factors on the $\mu$I sodium channel. *Neuron.* 7:775–785.